Multiresolution Analysis of Multiple Reflections in Transmission Lines

András Fehér[1], Ádám Békefi[2] and Szilvia Nagy[3]

Abstract – **Wavelet analysis is applied to time-domain signals of conducted measurements on cables with multiple reflections in order to detect repeating patterns in the time-frequency domain. In conducted radio frequency measurements the reflection is one of the most varying components of the measurement uncertainty.**

Keywords – **Reflection, wavelet analysis, measurement, measurement uncertainty.**

I. Introduction

In conducted radio measurements multiple reflections due to connections are always present, even if matched cables are used, and this effect plays an important role in the measurement uncertainty. In this article we present an analyzing method based on wavelet transform to study the nature of multiple reflections in a cable. The method is also tested with an artificially mis-matched cable, which has a part with 75 Ω impedance between two 50 Ω impedance pieces, without impedance matching.

II. On wavelet analysis

Wavelet analysis or multiresolution analysis [1–3] is a widely used tool in data processing, especially in image compression and noise reduction [4,5], but it can be also used for solving differential equations [6–8]. The results of the wavelet analysis can also detect patterns.

Let f be a function of the space of the square integrable functions $L^2(\mathbb{R})$. Wavelet analysis can be introduced e.g., as a generalization of the windowed Fourier transform

$$\mathcal{F}^{WFT}\{f\}(\tau,\omega)=\int w(t-\tau)f(t)\mathrm{e}^{-i\omega t}dt, \qquad (1)$$

and its discretised version

$$\mathcal{F}_{jk}^{WFT}\{f\}=a_{jk}^{WFT}=\int w(t-\tau_j)f(t)\mathrm{e}^{-i\omega_k t}dt. \qquad (2)$$

Here $w(t)$ is the window function, τ and ω are the time and angular frequency of the transformed signal, and j and k are the indices of the values resulting from the discrete transformation, belonging to $\tau_j = j\cdot\tau_0$ and $\omega_k = k\cdot\omega_0$, respectively. The reproduction, or synthesis of the original signal from its continuous transformed counterpart can be written as a double integral, similar to the original inverse Fourier integral, whereas the synthesis of the discrete windowed Fourier transformed signal from its coefficients is to be calculated as

$$f(t)\propto\sum_j\sum_k \bar{a}_{jk}^{WFT}\cdot\bar{w}_{jk}(t), \qquad (3)$$

where $\bar{w}_{jk}(t)$ is the basis function of the transformation

$$\bar{w}_{jk}(t)=\bar{w}(t-\tau_j)\cdot e^{i\omega_k t}, \qquad (4)$$

with overline meaning the complex conjugation. Using this notation, transformation (2) can be rewritten in a shortened form

$$\mathcal{F}_{jk}^{WFT}\{f\}=a_{jk}^{WFT}=\int w_{jk}(t)f(t)dt. \qquad (5)$$

The wavelet transform has similar formula, except that the transformation function is different, i.e., in case of discrete transformation

$$\mathcal{F}_{jk}^{WaT}\{f\}=d_{jk}=\int\psi_{jk}(t)f(t)dt. \qquad (6)$$

where the wavelets

$$\psi_{jk}(t)=2^{j/2}\psi(2^{-j}t-k). \qquad (7)$$

Similarly to the window functions, there are many types of wavelets, but once its type is chosen, all the wavelets are generated as scaled and shifted versions of one function, the mother wavelet $\psi(t)$. This means that while in case of the windowed Fourier transform, the envelop of the transforming function remains the same (only shifted in time), and increasing frequency manifests in more oscillations within the window function, in case of the wavelet transform the shape of the transforming function remains similar, only shrunk with the increasing frequency. A demonstration for the basis function shape can be seen in Fig. 1.

The inverse transformation takes the form

[1]Andras FEHÉR, Széchenyi István University, Radio Frequency Test Laboratory, Egyetem tér 1, Győr, Hungary, H-9026 E-mail: afeher@sze.hu. Web: http://rf.sze.hu

[2]Ádám BÉKEFI, Széchenyi István University, Department of Telecommunications, Egyetem tér 1, Győr, Hungary, H-9026 E-mail: bekefiadam@index.hu.

[3]Szilvia NAGY, Széchenyi István University, Department of Telecommunications, Egyetem tér 1, Győr, Hungary, H-9026 E-mail: nagysz@sze.hu.

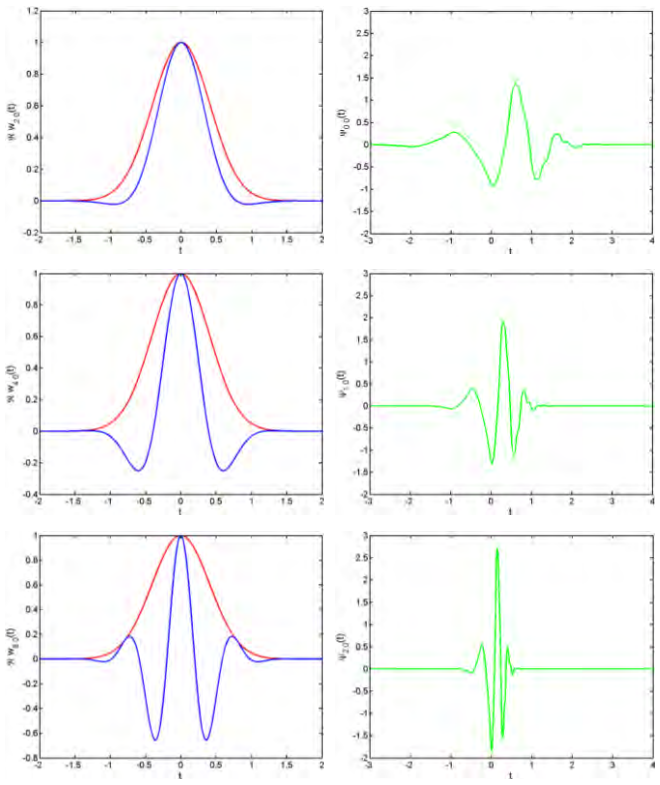

Fig. 1. Basis functions of a windowed Fourier transform (blue lines) with Gaussian window (red lines) and a wavelet (Daubechies-4, green lines) at three frequencies or resolution levels.

$$f(t) = \sum_{k=-\infty}^{\infty} c_{0k}\phi_{0k}(t) + \sum_{j=0}^{\infty}\sum_{k=-\infty}^{\infty} d_{jk}\psi_{jk}(t). \qquad (8)$$

In this equation the first summation is necessary to set the DC or low frequency components of the signal $f(t)$, whereas the second part makes the higher frequency refinements. The basis elements $\phi_{0k}(t)$ of the lowest frequency part are the scaling functions. They behave similarly to wavelets in Eq. (7). With increasing the frequency index j, the corresponding frequency doubles, as it can be seen from (7) and Fig. 1. It can also be observed in (7) that by increasing j by 1, the shift distance is halved. This property is very favourable if sharp edges, quick changes have to be reproduced, as near the changes the wavelet coefficients d_{jk} are large, and they are negligible in regions where smooth changes are present only. Such functions are often present both in image processing and in one dimensional data analysis, and they cannot be treated properly with windowed Fourier analysis, discrete cosine transform, etc., where the window width is constant, and usually much larger than the edge which is studied by it.

In practical applications, where a one or two dimensional digital (sampled and quantized) signal is analyzed, the highest frequency corresponds to the sampling frequency. During the analysis the vector (matrix in 2D) is transformed according to Fig. 2, consecutively. The frequency domain is always halved, the high-pass part will belong to the actual wavelets, the low pass one to the scaling functions; this can be further analyzed. Downsampling is needed, thus the total number of expanding coefficients remain constant after each step; $c_{j-1\,l}$ and $d_{j-1\,l}$ are half as long as the starting $c_{j\,l}$.

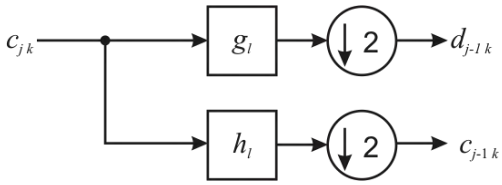

Fig. 2. Schematic diagram of one step in the wavelet analysis. Filter coefficients g_l and h_l represent the high-pass and low-pass filters, respectively; the circles mean downsampling by 2. The starting vector $c_{j\,k}$ can be either the original sampled signal or the low-pass output of the previous step.

The synthesis or reconstruction step is opposite to the analysis step plotted in Fig. 2.

III. Study of Multiple Reflections in Coaxial Cables

In order to study multiple reflections we have prepared a wrong connecting cable from Hirschmann KOKA 709 (75 Ω), and H155 (50 Ω) low loss coaxial cables. 50 Ω instruments were used for the measurement, and the connecting ends of the cable under test (CUT) were the H155 type lines, the middle part was substituted by 1.62 m of KOKA 709 line. As a reference high precision cable with attenuator was applied.

As a first step, the transmission characteristics of the cable was determined by a network analyzer; its parameter S21can be seen in Fig 3. A clear resonance valley is present at the first marker, near 105 MHz.

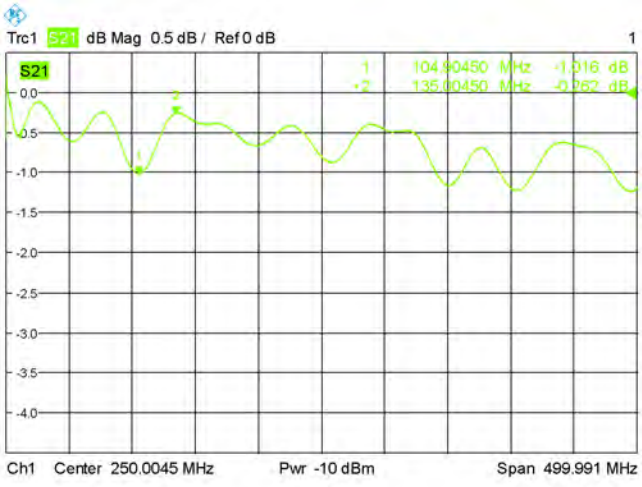

Fig. 3. S21 of the studied cable measured by Rohde&Schwarz ZVL Network Analyzer (9 kHz to 6 GHz)

As a test signal we have applied a carrier signal modulated by a 30 ns burst with a period of 200 ns. The carrier frequencies were near the 105 MHz point as the transmission

parameter varied there rather quickly, thus the modulated signals two sidebands had really different propagation conditions. Wavelet analysis is efficient where the quick changes in the time domain are present, hence the usage of the short bursts as modulator signals, practically the edges and their near environments are interesting. The cable was measured by a 5 GS/s Tectronix oscilloscope, an example with its reference signal can be seen in Fig. 4. The modulator and modulated signals were not synchronized in order to be able to study different relative phases, thus different shapes of

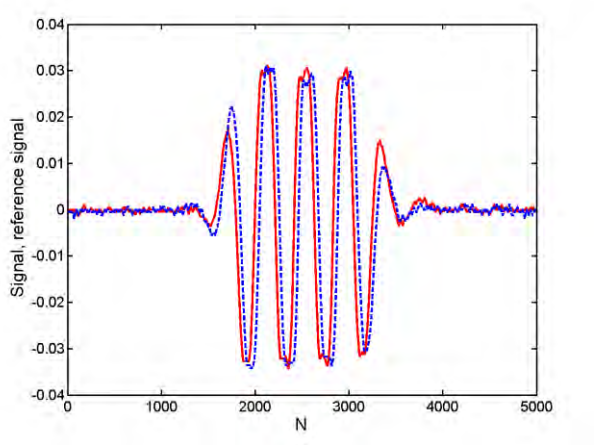

Fig. 4. An example of the measured signal with a carrier frequency of 120 MHz coming through the cable with reflection points (dashed blue line) and a reference cable (continuous red line). The horizontal axis is the number of the sampling.

signals.

Automatic measurement environment was prepared to gather sufficiently large number of data vectors, at the frequencies 93 MHz and 120 MHz. one hundred of measurements were carried out and wavelet transformed. The resulting coefficients varied a lot, as it is demonstrated in Fig. 5.

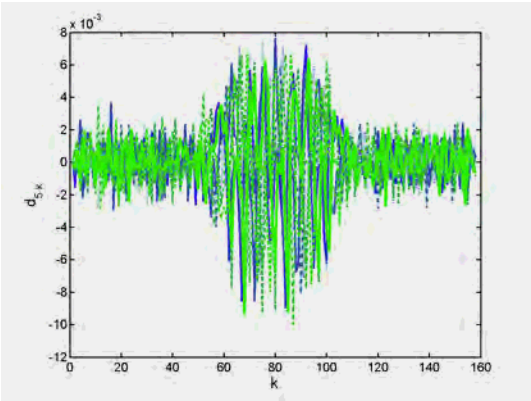

Fig. 5. The 5th wavelet transforms of 10 different signals from the cable with multiple reflection points.

In order to see the trends, the square of the coefficients d_{jk} were summarized for all the signals. The result's square root was normalized by the number of measurements,

$$\langle d_{jk} \rangle = \frac{\sqrt{\sum_{n=1}^{N_m} \left(d_{jk}^{[n]}\right)^2}}{N_m}, \qquad (9)$$

and plotted in Fig. 6 for $N_m = 10$ and $N_m = 100$. The upper index n means the serial number of the measurements, N_m the total number of measurements.

Fig. 7 contains the results for various resolution levels, i.e., for various frequency components. Ten analysing steps ($j = 0...9$) were carried out, but only those are given where interesting characteristics can be seen. The lower frequency

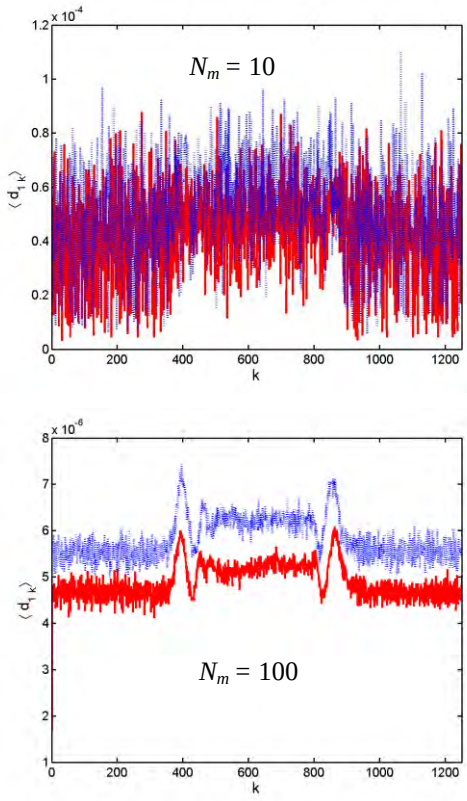

Fig. 6. The effective wavelet coefficients for 10 (upper subfigure) and 100 measurements. Data of cable with multiple reflection points is plotted with blue dashed line, the reference with red continuous line. Resolution index $j = 1$.

components do not differ significantly from the reference.

IV. Conclusion

The normalized wavelet coefficients of the reference and the multiple reflected signals can be distinguished in higher frequencies, however, the low frequency terms are in approximately the same, at least in average. The sampling time t_s = 400ps of the two-channel oscilloscope is just about 4 to 5 refinement steps away from the 93-120 MHz carrier frequency's characteristic time, thus the high frequency effects of the reflections and nonlinearities should be found in the first couple of steps, thus our results meet the expectations. Also, t_s becomes commensurable with the 30 ns

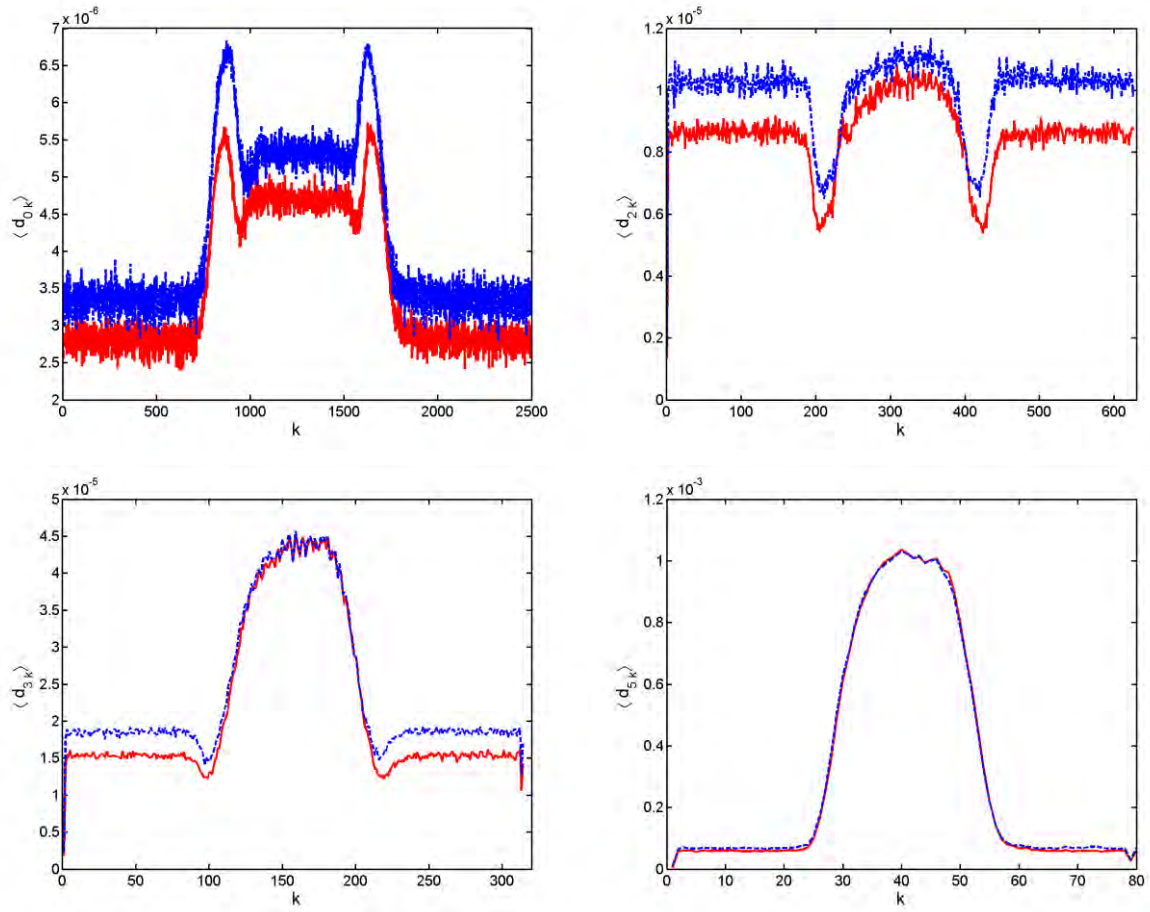

Fig. 7. The effective wavelet coefficients after 100 measurements.

burst time after 6-7 refinement steps, thus the lower frequency terms will contain mostly the burst itself. Multiple reflection in conducted measurements can be characterized by a significant increment in the average fine resolution wavelet coefficients.

ACKNOWLEDGEMENT

This work was supported by the Hegedüs Gyula fellowship and the projects TÁMOP-4.2.1./B-09/1/KONV-2010-0003, and TáMOP 4.1.1.A-10/1/KONV-2010-0005 of the Széchenyi István University.

REFERENCES

[1] I. Daubechies, Ten *Lectures on Wavelets*, CBMS-NSF Regional Conference Series in Applied Mathematics 61 (SIAM, Philadelphia, 1992).

[2] C. K. Chui, *An Introduction to Wavelets*, (Academic, San Diego, 1992).

[3] S. Mallat, *A theory for multiresolution signal decomposition: the wavelet representation*; IEEE Trans. Pattern Anal. Mach. Intel., vol. 11, pp. 674-693 (1989).

[4] J. Kaftan, A. A. Bell, C. Seiler, T. Aach, *Wavelet based denoising by correlation analysis for high dynamic range imaging*; IEEE International Conference on Image Processing, Cairo, pp. 3857-3860. (2009).

[5] C. Christopoulos, A. Skodras, and T. Ebrahimi, IEEE Trans. Consum. Electron. vol. 46, p. 1103 (2000).

[6] K. Urban, *Wavelet Methods for Elliptic Partial Differential Equations*, Oxford University Press, Oxford, (2009).

[7] W. Dahmen, *Wavelet methods for PDEs—Some recent developments*, J. Comput. Appl. Math. vol. 128, p. 133 (2001).

[8] J. Pipek, Sz. Nagy, *Refinement trajectory and determination of eigenstates by a wavelet based adaptive method*, J. Chem. Phys. vol. 125, 174107 (2006).

[9] M. Kuczmann, A. Iványi, *Finite Element Method in Magnetics*, Academic Press, Budapest, 2008, ISBN: 978 963 05 8649 8.